Journal of the Optical Society of America B
OPTICAL PHYSICS

Gain-induced Kerr beam cleaning in a femtosecond fiber amplifier

Henry Haig,[1,*] Nicholas Bender,[1] Yi-Hao Chen,[1] Anirban Dhar,[2] Nilotpal Choudhury,[2,3] Ranjan Sen,[3] Demetrios N. Christodoulides,[4] and Frank Wise[1]

[1]School of Applied and Engineering Physics, Cornell University, Ithaca, New York 14853, USA
[2]Fiber Optics and Photonics Division, CSIR-Central Glass and Ceramic Research Institute, Kolkata 700032, India
[3]Academy of Scientific and Innovative Research (AcSIR), Gaziabad 21002, India
[4]Ming Hsieh Department of Electrical and Computer Engineering, University of Southern California, Los Angeles, California 90089, USA
*tsh67@cornell.edu

Received 3 April 2023; revised 19 April 2023; accepted 24 April 2023; posted 24 April 2023; published 19 May 2023

Kerr beam cleaning is a nonlinear phenomenon in graded-index multimode fiber where power flows toward the fundamental mode, generating bell-shaped output beams. Here we study beam cleaning of femtosecond pulses accompanied by gain in a multimode fiber amplifier. Mode-resolved energy measurements and numerical simulations showed that the amplifier generates beams with high fundamental mode content (greater than 30% of the overall pulse energy) for a wide range of amplification levels. Control experiments using stretched pulses that evolve without strong Kerr nonlinear effects showed a degrading beam profile, in contrast to nonlinear beam cleaning. Temporal measurements showed that seed pulse parameters have a strong effect on the amplified pulse quality. These results may influence the design of future high-performance fiber lasers and amplifiers.

https://doi.org/10.1364/JOSAB.492262

1. INTRODUCTION

Multimode fiber guides light that has spatial and temporal degrees of freedom absent from light in single-mode fiber. These degrees of freedom potentially enable new capabilities and improved performance in fiber applications like telecommunications [1], imaging [2], and ultrafast lasers [3–5] that are limited by the properties of single-mode fiber. However, realizing the potential advantages of multimode fiber in ultrafast lasers is difficult, mainly due to the complexity of light propagation in multimode fiber. Linear effects like modal dispersion and mode coupling due to fiber defects make beams and pulses coming from multimode fiber difficult to predict and control. These dynamics become increasingly complex with high-power pulses that also experience nonlinear effects like four-wave mixing and cross-phase modulation.

Techniques to control the propagation of light in multimode fiber are therefore receiving significant research interest. Wavefront shaping is one widely used method [6–8], with various approaches that generally rely on either linear characterization of a medium [9–11] or a feedback mechanism to optimize a wavefront [12]. These methods are highly versatile, but are currently undesirable for certain applications because they require complicated and sometimes slow measurements, sensitive alignment, and sophisticated adaptive optics. Additionally, while feedback-based wavefront shaping schemes can tolerate nonlinearity [13–15], schemes based on the characterization of a medium are generally unsuitable for applications like ultrafast lasers where nonlinear effects are frequently significant. Alternatively, researchers are beginning to identify methods to control spatiotemporal fields in multimode fiber using nonlinear phenomena. Research in nonlinear multimode propagation and lasers is nascent, but attractor-like nonlinear phenomena have already been demonstrated in both passive fiber propagation [16,17] and multimode mode-locked oscillators [4,18,19]. These methods are limited, but have potential advantages over wavefront shaping techniques for certain applications where fixed beam profiles, speed, and simplicity are usually desired.

Kerr beam cleaning is one such nonlinear phenomenon [16], where interactions between transverse modes in a graded-index (GRIN) fiber drive energy toward the fundamental mode, creating a "cleaned" beam. This enables GRIN fiber to generate bell-shaped beams without adaptive optics, characterization, or feedback, and with low sensitivity to the alignment of the input light. Beam cleaning is natural to consider as a means to control the light in multimode fiber amplifiers, which could benefit from the large mode areas and increased dispersion of multimode fiber while still generating high-quality output beams. The phenomenon has been studied across a variety of regimes in passive fiber (nanosecond pulses [16], femtosecond pulses [20],

normal and anomalous [21] dispersion, and in spatiotemporally mode-locked lasers [4]). However, the impact of gain on beam cleaning is not fully understood. Recent studies demonstrate that beam cleaning of ∼500-ps pulses occurs in GRIN fiber amplifiers [22–24]. Unlike nanosecond-scale pulses, femtosecond pulses evolve with strong shaping from linear and nonlinear effects, and gain can deeply alter these evolutions (e.g., the self-similar attractor [25]). In general, nonlinear multimode fiber amplifiers and the interplay of spatiotemporal nonlinearity and gain remain largely unexplored.

In this paper, we study several aspects of femtosecond Kerr beam cleaning in a GRIN multimode fiber amplifier, with emphasis on spatial-profile dynamics. With mode-resolved energy measurements, we demonstrate that amplification can cause femtosecond pulses to undergo beam cleaning. Furthermore, we demonstrate that a nonlinear multimode amplifier can generate beams with a relatively high fundamental mode content (greater than 30%) for a wide range of amplification levels. Numerical simulations provide insight and model experimental results reasonably well. Control experiments with negligible Kerr nonlinearity show that multimode amplification tends to degrade beam profiles, and beam cleaning overcomes this effect. We also extended findings from a study of beam cleaning in double-clad fibers with ∼500-ps pulses [22] to the femtosecond regime and corroborate that beam cleaning in double-clad fiber can involve power transfer from cladding modes to core modes. Temporal measurements show that the output pulse quality depends strongly on the seed pulse properties, but suitably chosen seed pulses can be amplified to obtain compressible temporal profiles. These results demonstrate that nonlinear multimode fiber amplifiers can generate pulses with high-quality spatial and temporal profiles without sophisticated techniques like wavefront shaping, and may influence the design of future high-performance multimode lasers.

2. EXPERIMENTAL SETUP

A schematic of the experimental setup is shown in Fig. 1. Beam cleaning and amplification are studied in a GRIN fiber amplifier seeded by the output of a Yb fiber laser. A lens and three-axis translation stage couple the signal light into the GRIN fiber and adjust the input coupling conditions. We primarily focused on a co-pumped amplifier with a length of 1 m, but found similar behavior for counter-pumped amplifiers and fiber lengths between 1 and 2 m. The amplifier reached slope efficiencies near 10% and was pumped with up to 15 W. The fiber was loosely coiled to a diameter near 20 cm.

The Yb-doped GRIN fiber amplifier has a 30 μm core diameter and accommodates 20 guided core modes of a single polarization (40 total modes) according to numerical calculations [26]. The fiber was fabricated through a vapor-phase chelate delivery technique [27] to achieve a GRIN profile with uniform core doping and a peak Yb ion concentration of around 4000 ppm. The distribution of Al2O3 and Yb2O3 was nearly uniform along the length of the fiber. This fiber is identical to a fiber used in our previous study of spatiotemporal mode-locking [28]. The numerically calculated spatial modes of this fiber, along with normalized mode areas and overlap integrals, are shown in Fig. 2.

We measured mode energies of the output with off-axis digital holography [29]. This technique interferes a spatially invariant plane wave (reference beam) with an image of the fiber output face (object beam) on a CCD camera. The field of the object beam is then obtained by processing the Fourier transform of the interference pattern. An electronic variable delay stage scans the temporal overlap between reference and object beams and provides spectral resolution of the measured field. After measurement of the spatially and spectrally resolved field, the field is decomposed onto the numerically calculated fiber modes. This method does not measure the temporal profile of the output pulses, as relative phases between spectral components are not determined. For temporal measurements, the output pulses are compressed with a standard grating compressor and measured with a second-harmonic autocorrelator.

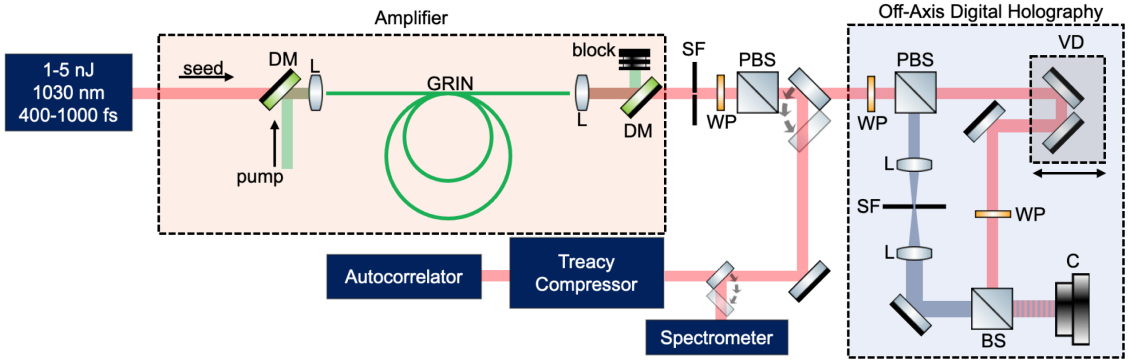

Fig. 1. GRIN fiber amplifier with mode-resolved measurements. The amplifier is pumped via a fiber-coupled 976 nm laser diode that is coupled into the fiber via a dichroic mirror (DM) and lens (L), which also couples the seed pulse from a Yb fiber laser. At the amplifier output, another dichroic mirror strips the signal of any remaining pump light and a circular spatial filter (SF) centered on the fiber core in a near-field plane blocks light in the cladding. A half-wave plate (WP) and polarizing beam splitter (PBS) isolate one polarization for analysis with temporal and spectral measurements in addition to mode-resolved energy measurements with an off-axis digital holography setup. The holography measurement consists of splitting the beam into reference (blue) and object (red) arms that are interfered on a camera (C). The reference arm is spatially filtered in the far-field plane to become plane-wave-like, while the object arm is subject to a variable delay (VD) to provide spectral resolution. The object arm images the fiber end facet to the camera, and blocking the reference arm allows direct near-field imaging of the fiber.

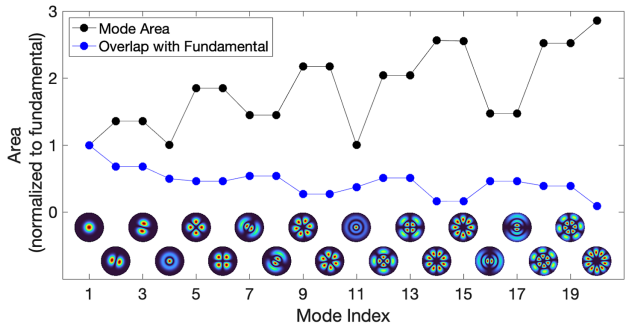

Fig. 2. Spatial mode properties (mode areas and overlap integrals with the fundamental mode) of the 20-mode GRIN fiber used here. The vertical axis is normalized to 51 μm^2, the fundamental mode area. Insets show intensity profiles of the modes.

These autocorrelations roughly represent a spatial average of the multimode temporal profiles, and are not an accurate full spatiotemporal measurement of the field.

The field correlations between the measured beams and mode-decomposed beams are typically above 90% for nonzero spectral components, which indicates accurate mode decomposition. We also estimated the uncertainty in mode occupation measurements by comparing field correlations between numerically generated mode superpositions with added mode amplitude errors. For the modes used here, average mode amplitude deviations of 5% correspond to fields with correlations between 70% and 90%. We conservatively assigned a 5% uncertainty to the mode energies here, and the primary conclusions we have drawn are valid for larger uncertainties (∼20%).

3. EXPERIMENTS: AMPLIFIED BEAM CLEANING

To look for visual indications of beam cleaning, we adjusted the input coupling under high pump power while monitoring the output beam. A wide range of spatial and temporal initial conditions produced cleaned beams. The spatial behavior of cleaned beams is similar for the entire range of input pulses used (energies between 1 and 5 nJ, durations between 150 and 1000 fs, and bandwidths between 4 and 20 nm centered at 1035 nm).

To study the behavior of beam cleaning with increasing gain, we performed mode-resolved energy measurements with an increasing pump power. Spatial and spectral measurements from this experiment are shown in Figs. 3 and 4. The 1 m amplifier was seeded with 1 nJ, 1 ps chirped pulses with a transform-limited duration near 300 fs. At low pump power, the output pulse has energy under 10 nJ. Low fundamental mode content (∼10%) and significant energy in higher-order mode groups gave the beam a complex shape. As the pump power was increased, the fundamental mode content increased, which concentrated the energy toward the center of the core and gave the beam a nearly circular shape. With further amplification, the fundamental mode content stayed high, fluctuating between 30% and 50% of the overall pulse energy as the pulse was amplified from 30 to over 200 nJ. Other initial conditions reproduced similar trends to the one shown here.

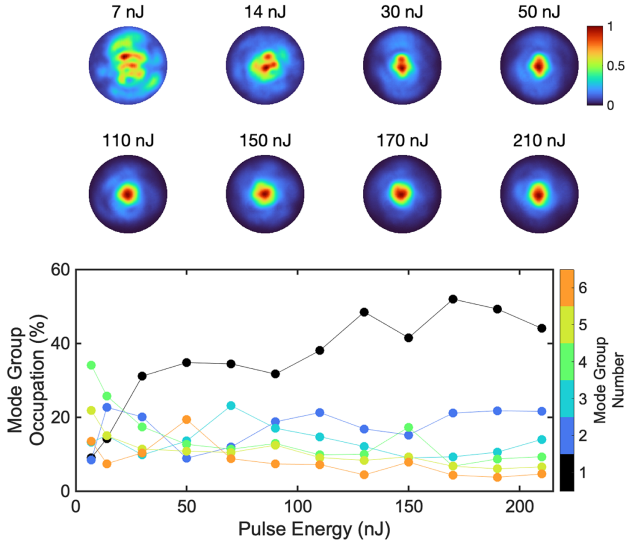

Fig. 3. Gain-induced beam cleaning in a GRIN fiber amplifier. The near-field beam profiles of the amplifier are seeded with 1 ps chirped pulses, with the increasing pump power and output pulse energy labeled above each beam profile. The colormap in the top-right panel is used for all other near-field images in this study. Plot below shows measured mode group occupations of the output pulses with beams shown above.

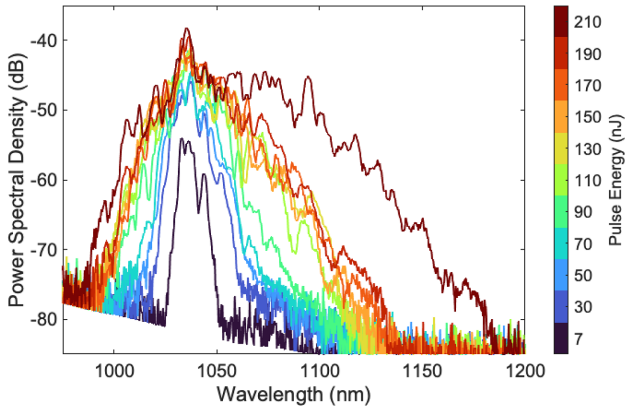

Fig. 4. Increasing amplification leads to increasingly nonlinear pulse evolutions. This is the spectra of the amplifier, for the initial condition shown in Fig. 3, with increasing pump power and output pulse energy. The multimode beam is coupled into a highly multimode fiber-coupled spectrometer, which measures a roughly spatially averaged spectrum and causes some of the modulations seen here.

Spectra for the same experiment are shown in Fig. 4. At a low pump power, the spectrum is similar to the seed spectrum but with additional modulation due to multimode interference in the spectrometer coupling fiber. As the pulse energy increases, the evolution becomes increasingly nonlinear and the spectrum broadens due to self- and cross- phase modulation. Above the highest pulse energy shown here, we began to observe indications of stimulated Raman scattering in the spectrum, so we will limit our discussion to pulse evolutions with only Kerr nonlinearity.

In this experiment, the nonlinear interactions that cause beam cleanup are driven by the increasing peak power of the

signal due to gain, rather than the peak power of the input. However, the behavior we observed was similar in several ways to passive beam cleaning [16,20,30]. The cleaned beams were visibly fundamental-mode-dominated with weak higher-order-mode backgrounds, similar to those reported in passive beam cleaning studies. The mode energy distributions of cleaned beams measured in Fig. 3 are qualitatively similar to those reported in a study of passive beam cleaning [30], with 30%–50% of the pulse energy in the fundamental mode and decreasing occupation with an increasing mode group number.

The behavior of gain-induced beam cleaning with increasing power is also similar to that of passive beam cleaning. In passive beam cleaning, increasing the pulse energy beyond the threshold for which beam cleaning first occurs results in no further significant changes to the mode energies, which is understood as irreversible thermalization [30]. We cannot make strict comparisons to a conservative thermodynamic theory since our system is not conservative. However, in our experiment the beam also remained cleaned and fundamental-mode-dominated with an increasing pulse energy. Past the initial threshold for cleaning, we observed only small changes to the beam profile and fundamental mode occupation that are evident in the mode occupancy measurements and near-field profiles shown in Fig. 3.

4. NUMERICAL SIMULATIONS

These experimental observations are modeled reasonably well by numerical simulations, demonstrating that gain induces beam cleaning. Our numerical model solves the generalized multimode nonlinear Schrödinger equation [31,32] with calculated modes of the fiber used here (Fig. 2) [26]. Gain was implemented with an adaptation of a steady-state model [33,34] that solved the Yb rate equations in both transverse and longitudinal spatial domains, with realistic absorption and emission cross sections. The details of this model will be the subject of a future publication. Simulations include the 20 core modes of the fiber with a single linear polarization.

Figure 5 shows the results of one representative simulation. The model amplifier was seeded with a 1 ps pulse with total energy above 0.5 nJ. The input coupling condition distributed 0.5 nJ equally across the first three mode groups (1/6 nJ for each mode group), 0.05 nJ in each mode from groups 4 and 5, and 0.005 nJ in each mode in group 6. This initial condition was similar to those reported in other studies of fs beam cleaning [20], and approximately models that of a Gaussian input beam that is not matched in diameter or centered to the fundamental mode. During propagation and amplification, [Fig. 5(b)], the fundamental mode occupancy increased as a result of nonlinear interactions with other modes. After 1 m, the fundamental mode obtained more than 45% of the overall pulse energy. The rest of the pulse energy was distributed roughly evenly across the other mode groups.

The simulation shown in Fig. 5 recreates basic aspects of our experiments (Fig. 3). However, strict comparison of a single simulation to an experiment is difficult due to the complexity of the nonlinear evolution and dependence on initial conditions. For this reason, we performed simulations that use a range of input conditions to understand the average behavior of the amplifier.

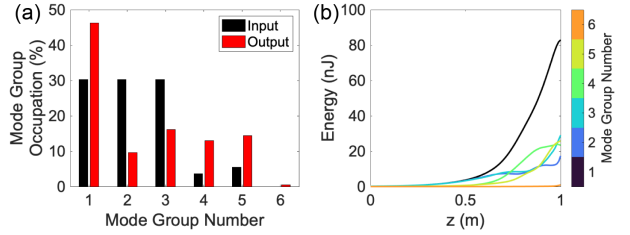

Fig. 5. Simulated beam cleaning for a particular input condition. (a) Input and output mode group occupations. (b) Mode group occupation evolution with longitudinal coordinate for the same initial condition as in (a).

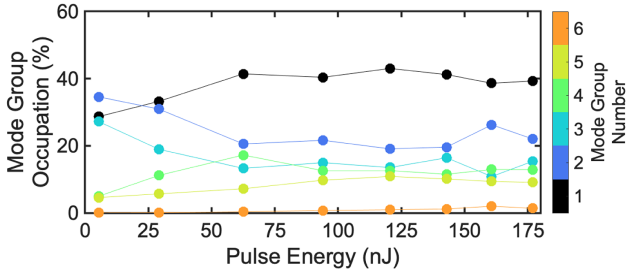

Fig. 6. Simulated beam cleaning for an ensemble average of initial conditions. Mode group occupation of the amplifier output pulse with increasing pump power and pulse energy. The data for each pulse energy are generated by averaging over five initial conditions that each have the same amplitude occupation but varying phases.

To generate the data shown in Fig. 6, the model amplifier was seeded with a set of five distinct initial conditions at a particular pump power. Each initial condition had the same mode occupancy distribution as in Fig. 5, but random phases between 0 and 2π were applied to each mode. For each pump power (pulse energy), the output mode energy distributions were recorded and averaged over the five initial conditions. The simulation results in Fig. 6 more closely model the trends shown in the experimental measurements in Fig. 3. Amplification-induced beam cleaning results in a high fundamental mode occupancy (∼40%) for a wide range of amplification levels. The occupation of higher-order mode groups generally decreases with increasing mode group index, similar to our experiment and studies of passive beam cleaning [30]

While these simulations model the general trends of experiments, we observed a discrepancy between the simulations and experiments in the magnitude of the fundamental mode content increase due to beam cleaning. In the experiments, the fundamental mode content increased by as much as 40%, while in the simulations we typically observed an increase of only 20%. Several aspects of the experiments are not accounted for in the simulations, and may be responsible for this discrepancy. First, more accurate modeling of the initial condition may be necessary to observe a larger increase in the fundamental mode content. Such modeling, however, is difficult because of linear mode coupling effects from fiber imperfections and bending, which are also not included in the simulations. While linear mode coupling is not expected to be strong for the short fiber here, even weak coupling has been shown to strongly impact beam cleaning dynamics [35,36]. Finally, we are unable to

include cladding modes in the simulations because there are thousands of such modes that would make the simulation runtimes prohibitively long. The experiments presented below suggest these modes surprisingly have a strong impact on beam cleaning in this fiber.

5. EXPERIMENTS: LINEAR AMPLIFICATION

To understand the spatial gain dynamics of the amplifier without Kerr nonlinear effects, we seeded the amplifier with highly chirped (400 ps) pulses. These pulses have similar energy and bandwidth to the other pulses used in this study, but their much lower peak power (∼10 W compared to ∼10 kW) ensures that nonlinear effects are negligible. Accurate mode decompositions of these long chirped pulses for their entire spectral range requires a much longer translation stage than the one available in our off-axis digital holography setup; therefore, for this particular experiment we relied only on visual inspection of the beam profiles and did not have quantitative mode energy measurements. Figure 7(a) shows beam profiles of the amplifier seeded with these pulses for increasing gain. At a low power, the input coupling was visually optimized to maximize the fundamental mode energy, which resulted in a fundamental-mode-dominated beam without significant higher-order mode background. Increasing the pump power degraded the beam quality, as higher-order-modes were amplified and the proportion of energy in the fundamental mode decreased.

This behavior contrasts strongly with that of the amplifier seeded with short pulses that evolved nonlinearly. To emphasize this, we included beam profiles in Fig. 7 from an experiment similar to the one shown in Fig. 3. In that case, the amplifier was seeded with short (400 fs) pulses that experienced strong nonlinear effects, with a different initial spatial condition than the experiment in Fig. 3. Unlike the amplifier seeded with low peak power pulses, the beam profile dramatically improved. Mode resolved energy measurements indicate that the fundamental mode content increases from below 10% to above 35% for a range of pulse energies from 30 to 165 nJ.

The degrading beam profiles shown in Fig. 7(a) suggest that the fundamental mode in GRIN fiber is unstable with gain in a uniformly doped core. This conclusion may be a consequence of the spatial properties of GRIN fiber modes, shown in Fig. 2. Higher-order modes have larger areas and experience larger gain than the fundamental mode. With an increasing mode number, the space occupied by a mode moves away from the core center and toward the core-cladding boundary. For beams with a high fundamental mode content, local gain saturation of the core center may be another mechanism that causes preferential amplification of higher-order modes over lower-order modes.

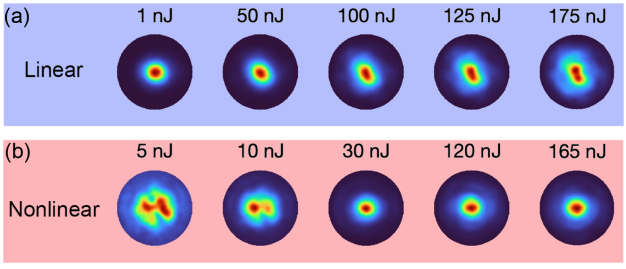

Fig. 7. Linear and nonlinear amplification in GRIN fiber. (a) Output beam profiles of the amplifier seeded with long (400 ps) pulses with low peak power (<10 W). (b) Output beam profiles of the amplifier seeded with short pulses (400 fs) with high peak power (>1 kW).

These experiments show that beam cleaning and gain have, in isolation, roughly opposite effects on mode energy distributions: Beam cleaning drives power toward a mode distribution dominated by lower-order modes, while gain amplifies all modes and disrupts the amplification of fundamental-mode-dominated beams. For the parameter range used here, beam cleaning overcomes the opposing effect of gain to generate and sustain fundamental-mode-dominated beams for a wide range of gain levels.

6. EXPERIMENTS: CLADDING MODES

Previous work on beam cleaning of nanosecond-scale pulses indicates that cladding modes can play a significant role in beam cleaning in double-clad fiber [22]. This study showed that beam cleaning taking place in an unpumped double-clad fiber amplifier is accompanied by significant energy transfer from cladding modes to core modes. Details of this process are unclear, but a potential explanation is that beam cleaning occurs across the entire fiber structure, which has a GRIN core and step-index cladding.

This result is surprising for several reasons. First, beam cleaning occurs in GRIN fiber due to the equally spaced mode propagation constants, which support efficient four-wave mixing. The modes of step-index guiding structures, like the claddings of double-clad fibers, do not have this eigenvalue spectrum [30]. Consequently, beam cleaning has not been observed in step-index fiber (except for four-wave mixing, which can be similar to cleaning, for particular mode distributions in few-mode step-index fiber [37]). Additionally, nonlinear effects in cladding modes are much weaker than in core modes since cladding modes typically have mode areas over an order of magnitude larger than core modes.

To study the impact of cladding modes on beam cleaning of fs pulses, we performed a similar experiment to the one presented in [22] that uses ∼500-ps pulses, but with femtosecond pulses. With the pump off, we seeded the fiber with a 250 fs pulse of energy up to 200 nJ. We intentionally coupled most of the light into the cladding by moving the fiber out of the focal plane of the input-coupling lens. Figure 8 shows the output beam profiles with increasing input energy from 1 to 200 nJ. The beam profile exhibits clear signatures of beam cleaning in the core, despite a small absorption due to the Yb doping. In this case, cleaning occurred due to the high peak power of the input signal alone, without the assistance of gain. The beam profiles have a blurred background due to the significant energy present in cladding modes.

Using a spatial filter on an image plane of the fiber output, as shown in Fig. 1, we measured the fraction of light present in the core as the input pulse energy was increased. Similar to [22], we found that the total fraction of light in the core region can increase significantly as the pulse energy increases, from 15% to 33%. Signal absorption due to the Yb-doped core is not responsible for this increase, since the total power transmission of the fiber remains nearly constant. This suggests that beam cleaning

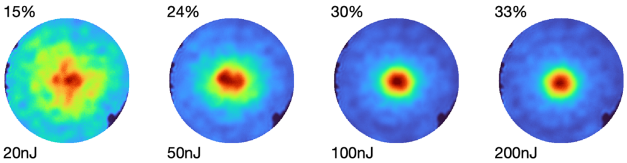

Fig. 8. Cladding modes impact beam cleaning. Near-field beam profiles of passive beam cleaning in the unpumped Yb doped fiber. A large fraction of the input light is intentionally coupled to the cladding, which causes the blurred backgrounds in each profile. The fraction of the overall pulse energy confined to the core region is listed above each beam profile, and the overall pulse energy is listed below. The edges of the profiles partially show the edge of the iris spatial filter used to measure the light in the core.

occurs both within the GRIN fiber core and across the fiber index structure that has both GRIN and step-index regions. As suggested in [22], leaky modes near the core-cladding boundary may contribute to this effect. The energies and peak powers at which beam cleaning occurs (several 10s of kW) are similar or slightly higher than those reported in other femtosecond beam cleaning studies [20], which may be a consequence of much of the light occupying large cladding modes. This result supplements our main experiments and corroborates another study of amplified beam cleaning [22]. A full understanding of this phenomenon is beyond the scope of this work and deserves additional study.

7. EXPERIMENTS: TEMPORAL PROFILES

The temporal evolution of femtosecond pulses in multimode fiber is highly complicated due to an array of linear and nonlinear spatiotemporal effects [31] and their interaction. Briefly, as pulses propagate in multimode fiber, each mode experiences a different group velocity (modal walk-off). Energy and phase information is nonlinearly exchanged between modes depending on the spatial, temporal, and spectral overlaps of the modes along with phase-matching constraints imposed by modal propagation constants. Our experiments and simulations indeed indicate that the temporal dynamics of beam cleaning and gain are complex, and are more difficult to interpret than the spatial dynamics. We observed beam cleaning with a range of spatial input coupling conditions and seeded pulses with various temporal and spectral properties. Cleaned beams resulting from different amplifier inputs are similar both in appearance and mode energy distribution [e.g., Figs. 3 and 7(b)]. Unlike the amplifier spatial profiles, output temporal profiles have a strong dependence on the temporal properties of the input pulse. Despite this complexity, we found that it is possible to generate reasonably high-quality pulses that have undergone beam cleaning by configuring the seed and amplifier to both limit nonlinear phase accumulation and reduce the effect of linear walk-off between modes. We demonstrated this here by a comparison of two different seed and amplifier configurations, as shown in Fig. 9.

Figure 9(a) shows a beam-cleaned amplified pulse when the amplifier is arranged in a co-pumping configuration, and seeded with short (150 fs), transform-limited pulses with a relatively broad bandwidth (>10 nm). For this input pulse duration, at low and high power (before and after cleaning occurs, respectively), the output pulse can only be compressed to near twice the transform-limited duration. The peak power of the input pulse is high (>10 kW) and the gain is strongest at the beginning of the fiber due to the co-pumping configuration. These factors ensure large nonlinear phase accumulation, which is estimated as $\sim 3\pi$ for the 29 nJ output pulse here. This estimation was made by simulating a single-mode amplifier with a mode area equivalent to the fundamental mode of the multimode fiber used here. The linear delay between adjacent mode groups over one meter was small (~20 fs) compared to the input pulse duration, but the delay between nonadjacent mode groups ($\gtrsim$50 fs) was a significant fraction of the input pulse duration. Modal walk-off and its interplay with four-wave mixing and cross-phase modulation therefore played a significant role in shaping the pulse. For this input coupling condition, we also observed a reduction in the pedestal structure that accompanies beam cleaning, which is evident in Fig. 9(a). This is reminiscent of work demonstrating temporal compression of nanosecond pulses undergoing beam cleaning [38], but we suspect this behavior is incidental to the particular input condition used here rather than a fundamental phenomenon.

Figure 9(b) shows output temporal profiles of the amplifier seeded with narrow bandwidth (2 nm), slightly chirped pulses with a 1 ps duration. At both low and high pulse energies, the output pulses are compressible to near the transform-limited duration with a small pedestal structure. The high-power pulse compresses to a shorter duration than the low-power pulse due to nonlinear spectral broadening during propagation. This configuration yields a lower nonlinear phase accumulation than the previous example due to both the lower peak-power of the seed pulse (~kW) and the counter-pumping configuration, which imparts the end of the fiber with higher gain than the beginning. We also estimated the total nonlinear phase accumulation as $\sim 3\pi$, but the output pulse was cleaner and nearly three times as energetic as the previous example. For this seed duration, linear walk-off between modes and mode groups was a small (<10%) fraction of the pulse duration, so modal walk-off played only a small role in shaping the pulse.

These results show that by choosing appropriate seed pulses, it is possible to design multimode amplifiers that generate reasonably high-quality temporal and spatial profiles without requiring sophisticated wavefront shaping. In particular, pulses with longer durations and narrower bandwidths obtain higher energy and pulse quality than shorter, more broadband seed pulses. This is a consequence of a lower nonlinear phase accumulation and the diminished impact of linear modal walk-off for pulses with a duration much greater than modal delay. The autocorrelations in Fig. 9 show the highest peak-power pulses we obtained for a given seed pulse. Amplifying the pulses beyond the energies shown here results in strong nonlinear deterioration of the temporal profile, but only small changes to the beam profiles, which remain fundamental-mode-dominated, as shown in Fig. 3. We suspect that higher-energy pulses that undergo beam cleaning can be obtained by further temporal stretching of the seed pulses.

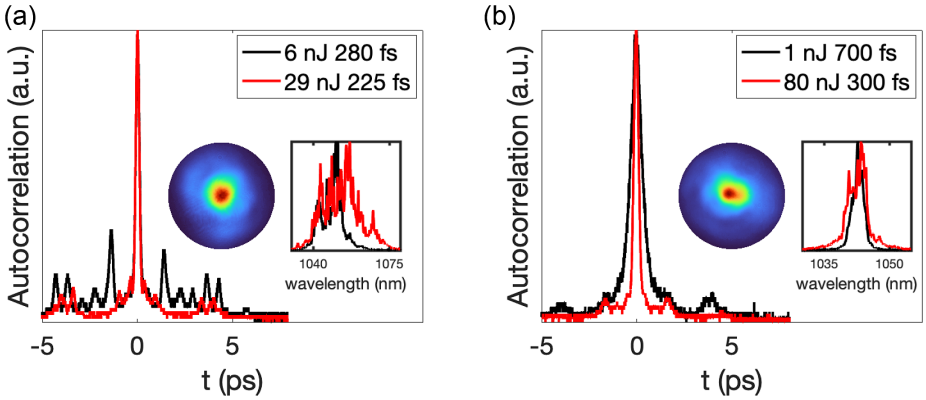

Fig. 9. Output temporal profiles for different seed pulses and pumping configurations. (a) Autocorrelation of the co-pumped amplifier output at low (black) and high (red) power, seeded with short (150 fs) pulses. The central peak of both pulses strongly overlaps. Insets show the high-power, cleaned beam profile and the spectra at low and high power (black and red, respectively). (b) The same measurements as (a) with a counter-pumped amplifier seeded with a narrow bandwidth (2 nm) chirped seed pulse.

8. CONCLUSION

We presented experimental observations of beam cleaning of femtosecond pulses caused by amplification. We found that beam cleaning induced by gain is qualitatively similar to beam cleaning that occurs in passive fiber, and mode-resolved measurements and numerical simulations verify high fundamental mode content (>30%) for a wide range of amplification levels. Control experiments where the amplifier was seeded by low peak-power pulses showed that the gain in GRIN fiber degrades fundamental-mode-dominated beam profiles, while beam cleaning overcomes this effect to generate and sustain beams with high fundamental mode content. The impact of cladding modes on beam cleaning in double-clad fiber was briefly studied, and we found that cladding modes can transfer a large amount of energy to core modes. Temporal measurements show that the seed pulse properties have a strong impact on the output temporal pulse quality. High-quality output pulses are obtained by choosing seed pulses that limit nonlinear phase accumulation and experience only small mode walk-off effects.

These results are a step toward multimode fiber lasers that generate high-quality beams without wavefront shaping. Ultimately, the utility of multimode amplifiers will be measured against single-mode amplifiers. The doped GRIN fiber available to us has a relatively small core (30 μm) and fundamental mode (10 μm), and the amplifier performance here does not exceed that available from modern single-mode nonlinear amplifiers [39]. However, it may be possible to apply these findings to larger fibers and obtain pulses that exceed the performance available from single-mode nonlinear amplifiers. Our observations suggest that the spatial and temporal behavior of beam cleaning are somewhat independent, because a similar spatial behavior is observed for a variety of different temporal behaviors. This supports the idea that beam cleaning is primarily a spatial phenomenon, which is corroborated by observations of beam cleaning across time scales [4,16,20], and the success of CW theoretical descriptions [30]. Therefore, we suspect it will be possible to design amplifiers that accommodate both beam cleaning and advantageous nonlinear evolutions, like the self-similar evolution [25], nonlinear chirped pulse amplification [40], or other currently unknown multimode evolutions. Development of such sources will require further study of the temporal behavior of nonlinear multimode amplification, and will benefit from larger core, more highly multimode gain fibers.

Funding. National Science Foundation (ECCS-1912742); Office of Naval Research (N00014-20-1-2789); Simons Foundation (733682)

Acknowledgment. The authors would like to thank Yuhang Wu and Yishai Eisenberg for helpful discussions related to this work.

Disclosures. The authors declare no conflicts of interest.

Data availability. Data underlying the results presented in this paper are not publicly available at this time but may be obtained from the authors upon reasonable request.

REFERENCES

1. D. J. Richardson, J. M. Fini, and L. E. Nelson, "Space-division multiplexing in optical fibres," Nat. Photonics **7**, 354–362 (2013).
2. T. čižmár and K. Dholakia, "Shaping the light transmission through a multimode optical fibre: complex transformation analysis and applications in biophotonics," Opt. Express **19**, 18871–18884 (2011).
3. L. G. Wright, D. N. Christodoulides, and F. W. Wise, "Spatiotemporal mode-locking in multimode fiber lasers," Science **358**, 94–97 (2017).
4. U. Tegin, B. Rahmani, E. Kakkava, D. Psaltis, and C. Moser, "Single-mode output by controlling the spatiotemporal nonlinearities in mode-locked femtosecond multimode fiber lasers," Adv. Photon. **2**, 056005 (2020).
5. X. Wei, J. C. Jing, and Y. Shen, "Harnessing a multi-dimensional fibre laser using genetic wavefront shaping," Light Sci. Appl. **9**, 149 (2020).
6. A. P. Mosk, A. Lagendijk, G. Lerosey, and M. Fink, "Controlling waves in space and time for imaging and focusing in complex media," Nat. Photonics **6**, 283–292 (2012).
7. H. Cao, A. P. Mosk, and S. Rotter, "Shaping the propagation of light in complex media," Nat. Phys. **18**, 994–1007 (2022).
8. S. Gigan, O. Katz, H. B. de Aguiar, *et al.*, "Roadmap on wavefront shaping and deep imaging in complex media," J. Phys. Photon. **4**, 042501 (2022).
9. S. M. Popoff, G. Lerosey, R. Carminati, M. Fink, A. C. Boccara, and S. Gigan, "Measuring the transmission matrix in optics: An approach to the study and control of light propagation in disordered media," Phys. Rev. Lett. **104**, 100601 (2010).
10. J. Carpenter, B. J. Eggleton, and J. Schröder, "110 × 110 optical mode transfer matrix inversion," Opt. Express **22**, 96–101 (2014).

11. W. Xiong, P. Ambichl, Y. Bromberg, B. Redding, S. Rotter, and H. Cao, "Spatiotemporal control of light transmission through a multimode fiber with strong mode coupling," Phys. Rev. Lett. **117**, 053901 (2016).
12. I. M. Vellekoop, "Feedback-based wavefront shaping," Opt. Express **23**, 12189–12206 (2015).
13. T. Omer, A. M. Caravaca-Aguirre, K. Wagner, and R. Piestun, "Adaptive wavefront shaping for controlling nonlinear multimode interactions in optical fibres," Nat. Photonics **12**, 368–374 (2018).
14. R. Florentin, V. Kermene, A. Desfarges-Berthelemot, and A. Barthelemy, "Space-time adaptive control of femtosecond pulses amplified in a multimode fiber," Opt. Express **26**, 10682–10690 (2018).
15. E. Deliancourt, M. Fabert, A. Tonello, K. Krupa, A. Desfarges-Berthelemot, V. Kermene, G. Millot, A. Barthélémy, S. Wabnitz, and V. Couderc, "Wavefront shaping for optimized many-mode Kerr beam self-cleaning in graded-index multimode fiber," Opt. Express **27**, 17311–17321 (2019).
16. K. Krupa, A. Tonello, B. M. Shalaby, M. Fabert, A. Barthélémy, G. Millot, S. Wabnitz, and V. Couderc, "Spatial beam self-cleaning in multimode fibres," Nat. Photonics **11**, 237–241 (2017).
17. L. G. Wright, Z. Liu, D. A. Nolan, M.-J. Li, D. N. Christodoulides, and F. W. Wise, "Self-organized instability in graded-index multimode fibres," Nat. Photonics **10**, 771–776 (2016).
18. L. G. Wright, P. Sidorenko, H. Pourbeyram, Z. M. Ziegler, A. Isichenko, B. A. Malomed, C. R. Menyuk, D. N. Christodoulides, and F. W. Wise, "Mechanisms of spatiotemporal mode-locking," Nat. Phys. **16**, 565–570 (2020).
19. U. Teğin, E. Kakkava, B. Rahmani, D. Psaltis, and C. Moser, "Spatiotemporal self-similar fiber laser," Optica **6**, 1412–1415 (2019).
20. Z. Liu, L. G. Wright, D. N. Christodoulides, and F. W. Wise, "Kerr self-cleaning of femtosecond-pulsed beams in graded-index multimode fiber," Opt. Lett. **41**, 3675–3678 (2016).
21. Y. Wu, H. Pourbeyram, D. N. Christodoulides, and F. W. Wise, "Weak beam self-cleaning of femtosecond pulses in the anomalous dispersion regime," Opt. Lett. **46**, 3312–3315 (2021).
22. R. Guenard, K. Krupa, R. Dupiol, M. Fabert, A. Bendahmane, V. Kermene, A. Desfarges-Berthelemot, J. L. Auguste, A. Tonello, A. Barthélémy, G. Millot, S. Wabnitz, and V. Couderc, "Kerr self-cleaning of pulsed beam in an ytterbium doped multimode fiber," Opt. Express **25**, 4783–4792 (2017).
23. A. Niang, D. Modotto, A. Tonello, F. Mangini, U. Minoni, M. Zitelli, M. Fabert, M. A. Jima, O. N. Egorova, A. E. Levchenko, S. L. Semjonov, D. S. Lipatov, S. Babin, V. Couderc, and S. Wabnitz, "Spatial beam self-cleaning in tapered Yb-doped grin multimode fiber with decelerating nonlinearity," IEEE Photon. J. **12**, 6500305 (2020).
24. M. A. Jima, A. Tonello, A. Niang, T. Mansuryan, K. Krupa, D. Modotto, A. Cucinotta, V. Couderc, and S. Wabnitz, "Numerical analysis of beam self-cleaning in multimode fiber amplifiers," J. Opt. Soc. Am. B **39**, 2172–2180 (2022).
25. M. E. Fermann, V. I. Kruglov, B. C. Thomsen, J. M. Dudley, and J. D. Harvey, "Self-similar propagation and amplification of parabolic pulses in optical fibers," Phys. Rev. Lett. **84**, 6010–6013 (2000).
26. A. B. Fallahkhair, K. S. Li, and T. E. Murphy, "Vector finite difference modesolver for anisotropic dielectric waveguides," J. Lightwave Technol. **26**, 1423–1431 (2008).
27. N. Choudhury, N. K. Shekhar, A. Dhar, and R. Sen, "Graded-index ytterbium-doped optical fiber fabricated through vapor phase chelate delivery technique," Phys. Status Solidi A **216**, 1900365 (2019).
28. H. Haig, P. Sidorenko, A. Dhar, N. Choudhury, R. Sen, D. Christodoulides, and F. Wise, "Multimode Mamyshev oscillator," Opt. Lett. **47**, 46–49 (2022).
29. E. Cuche, P. Marquet, and C. Depeursinge, "Spatial filtering for zero-order and twin-image elimination in digital off-axis holography," Appl. Opt. **39**, 4070–4075 (2000).
30. H. Pourbeyram, P. Sidorenko, F. O. Wu, N. Bender, L. Wright, D. N. Christodoulides, and F. Wise, "Direct observations of thermalization to a Rayleigh–Jeans distribution in multimode optical fibres," Nat. Phys. **18**, 685–690 (2022).
31. F. Poletti and P. Horak, "Description of ultrashort pulse propagation in multimode optical fibers," J. Opt. Soc. Am. B **25**, 1645–1654 (2008).
32. L. G. Wright, Z. M. Ziegler, P. M. Lushnikov, Z. Zhu, M. A. Eftekhar, D. N. Christodoulides, and F. W. Wise, "Multimode nonlinear fiber optics: Massively parallel numerical solver, tutorial, and outlook," IEEE J. Sel. Top. Quantum Electron. **24**, 1–16 (2018).
33. S. K. Turitsyn, A. E. Bednyakova, M. P. Fedoruk, A. I. Latkin, A. A. Fotiadi, A. S. Kurkov, and E. Sholokhov, "Modeling of CW Yb-doped fiber lasers with highly nonlinear cavity dynamics," Opt. Express **19**, 8394–8405 (2011).
34. R. Lindberg, P. Zeil, M. Malmström, F. Laurell, and V. Pasiskevicius, "Accurate modeling of high-repetition rate ultrashort pulse amplification in optical fibers," Sci. Rep. **6**, 34742 (2016).
35. O. S. Sidelnikov, E. V. Podivilov, M. P. Fedoruk, and S. Wabnitz, "Random mode coupling assists Kerr beam self-cleaning in a graded-index multimode optical fiber," Opt. Fiber Technol. **53**, 101994 (2019).
36. J. Garnier, A. Fusaro, K. Baudin, C. Michel, K. Krupa, G. Millot, and A. Picozzi, "Wave condensation with weak disorder versus beam self-cleaning in multimode fibers," Phys. Rev. A **100**, 053835 (2019).
37. Z. Mohammadzahery, M. Jandaghi, E. Aghayari, and H. Nabavi, "Observation of spatial nonlinear self-cleaning in a few-mode step-index fiber for special distributions of initial excited modes," Sci. Rep. **11**, 24350 (2021).
38. K. Krupa, A. Tonello, V. Couderc, A. Barthélémy, G. Millot, D. Modotto, and S. Wabnitz, "Spatiotemporal light-beam compression from nonlinear mode coupling," Phys. Rev. A **97**, 043836 (2018).
39. P. Sidorenko, W. Fu, and F. Wise, "Nonlinear ultrafast fiber amplifiers beyond the gain-narrowing limit," Optica **6**, 1328–1333 (2019).
40. S. Zhou, L. Kuznetsova, A. Chong, and F. W. Wise, "Compensation of nonlinear phase shifts with third-order dispersion in short-pulse fiber amplifiers," Opt. Express **13**, 4869–4877 (2005).